EDGE ARTICLE

Check for updates

Carbazolylgold(III) complexes with thermally activated delayed fluorescence switched on by ligand manipulation as high efficiency organic light-emitting devices with small efficiency roll-offs†

Chun-Yin Wong, [a] Man-Chung Tang, [a] Lok-Kwan Li, [a] Ming-Yi Leung, [ab] Wai-Kit Tang, [a] Shiu-Lun Lai, [a] Wai-Lung Cheung, [a] Maggie Ng, [a] Mei-Yee Chan *[ab] and Vivian Wing-Wah Yam *[ab]

A series of carbazolyl ligands has been designed and synthesized through the integration of various electron-donating and electron-accepting motifs, including electron-donating 4-(diphenylamino)aryl and electron-accepting cyano and diphenylphosphine oxide moieties, for the development of a new class of gold(III) complexes, where the energies of their triplet intraligand and ligand-to-ligand charge transfer excited states can be manipulated for the activation of thermally activated delayed fluorescence (TADF). Upon excitation, these complexes show high photoluminescence quantum yields of up to 80% in solid-state thin films, with short excited state lifetimes down to 1 μs. Vacuum-deposited and solution-processed organic light-emitting devices based on these complexes demonstrate promising electroluminescence (EL) performance with maximum external quantum efficiencies of 15.0% and 11.7%, respectively, and notably small efficiency roll-off values of less than 1% at the practical luminance brightness level of 1000 cd m^{-2}. These distinct EL performances are believed to be due to the occurrence of multichannel radiative decay pathways *via* both phosphorescence and TADF that significantly shorten the emission lifetimes and hence reduce the occurrence of the detrimental triplet–triplet annihilation in the gold(III) complexes.

Introduction

Organic light-emitting devices (OLEDs) have been widely utilized in modern electronic displays, including mobile phones, augmented reality and virtual reality equipment, and 8K televisions owing to their excellent color gamut, fast response time, wide viewing angle and self-emissive capability.[1–4] Thermally activated delayed fluorescence (TADF)

aInstitute of Molecular Functional Materials, Department of Chemistry, The University of Hong Kong, Pokfulam Road, Hong Kong, P. R. China. E-mail: wwyam@hku.hk; chanmym@hku.hk; Fax: +852-2857-1586; Tel: +852-2859-2153

bHong Kong Quantum AI Lab Limited, 17 Science Park West Avenue, Pak Shek Kok, Hong Kong, P. R. China

† Electronic supplementary information (ESI) available: Synthetic route to carbazolylgold(III) complexes; thermogravimetric analysis; cyclic voltammograms; electrochemical data; UV-vis absorption spectra; absorption data; transient absorption spectra; PL spectra in solid-state thin films; selected structural parameters of the ground-state geometries; TDDFT/CPCM orbital and excitation energies; simulated absorption spectra; spatial plots of selected frontier MOs; orbital energy diagrams; natural transition orbital pairs; Cartesian coordinates; molecular orientation parameters; EL spectra, EQEs and lifetime data of gold(III) OLEDs. See https://doi.org/10.1039/d2sc03037c

compounds have received increasing attention as they can serve as an alternative to phosphorescent metal complexes, mainly because of their capability of harvesting all singlet and triplet excitons to achieve 100% internal quantum efficiency for light generation through the up-conversion of triplet excitons to singlet excitons *via* reverse intersystem crossing (RISC) to generate delayed fluorescence.[5] However, long-lived triplet excitons that are usually associated with organic emitters with lifetimes in the range of hundreds of microseconds to milliseconds will accumulate in the narrow recombination zone at high current densities, inevitably leading to severe triplet–triplet annihilation (TTA), exciton–polaron annihilation, *etc.*[6–10] This will result in severe efficiency roll-offs observed at a high practical brightness of around 1000–50 000 cd m^{-2}, hindering their applications in displays and outdoor lighting systems.[11–13] As the presence of the heavy metal center is known to enhance spin–orbit coupling (SOC), which can increase the rate of intersystem crossing (ISC)[14,15] and also RISC,[16] there has been a growing interest in metal-containing TADF emitters in recent years. Due to the shorter delayed fluorescence lifetimes of metal-TADF emitters,[17] it is envisaged that they can replace organic TADF molecules to overcome the unwanted efficiency

roll-offs. Moreover, cyclometalated metal complexes usually possess higher thermal stabilities,[18] which can improve the operational lifetimes of OLEDs. Early reports on metal-TADF emitters are mostly based on copper(I) systems.[19–21] Although copper(I) complexes have relatively lower thermal stabilities,[22] their TADF OLEDs have been found to show rather attractive external quantum efficiencies (EQEs),[23,24] providing the impetus for the development of metal-TADF emitters. Since then, various classes of metal-TADF emitters based on palladium(II),[25,26] silver(I),[17,27–29] gold(I)[30,31] and gold(III) systems[32–37] have been designed and synthesized. Of particular interest are examples involving tetradentate ligand-containing palladium(II) complexes that were reported to show phosphorescence and delayed fluorescence simultaneously.[25] These devices demonstrate maximum EQEs of 20.9% with operational lifetimes (LT$_{90}$) of over 20 000 hours at 100 cd m^{-2}.[25] Carbene metal amides with silver(I)[27] and gold(I)[30] as the metal centers have also been reported as metal-TADF emitters, where maximum EQEs of 13.7% and 27.5% have been achieved, respectively.

Apart from copper(I), silver(I) and gold(I) emitters, gold(III) emitters have also been attracting a lot of attention since 2005.[38,39] A variety of cyclometalating C^N^C[40–42] and C^C^N gold(III) complexes[43,44] and tetradentate gold(III) complexes[45,46]

showing high performances and a wide range of emission colours have been reported. Since 2017, gold(III) emitters have also been reported to show TADF behavior, including alkynylgold(III)[33,35] and arylgold(III) C^N^C complexes,[32] carbazolylgold(III) C^C^N complexes[36,37] and tetradentate gold(III) complexes.[34] All of them are found to exhibit promising electroluminescence (EL) performance with maximum EQEs reaching 25%. These findings demonstrate the possibility of the realization of high efficiency and robust metal-TADF emitters for OLED applications. Recently, new classes of alkynylgold(III) C^N^C complexes[35] and carbazolylgold(III) C^C^N complexes with thienopyridine and thienoquinoline moieties in the pincer ligand[37] have been demonstrated as metal-containing TADF emitters. Based on our development of various cyclometalating C^C^N ligand-containing carbazolylgold(III) complexes,[36,37,43,44] instead of modifying the pincer ligand, a new class of carbazolylgold(III) complexes with different ancillary ligands has been designed and synthesized. Specifically, substituted carbazolyl ligands with various electron-donating and electron-accepting moieties have been incorporated into the gold(III) precursor complex to yield complexes **1–6**, as shown in Chart 1. The judicious choices of 4-(diphenylamino)aryl, cyano and diphenylphosphine oxide moieties at the 2- and 3-positions of the
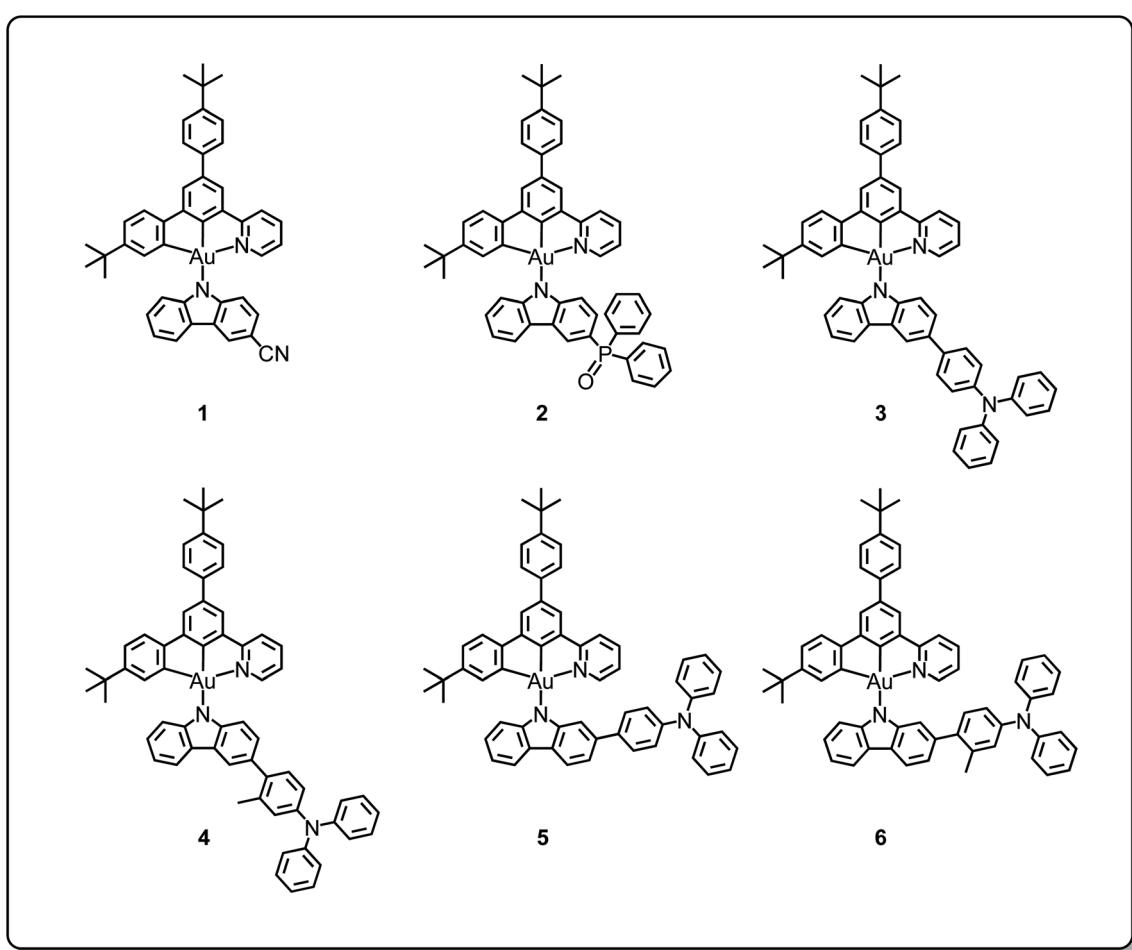
Chart 1 Molecular structures of carbazolylgold(III) complexes.

carbazole have allowed the manipulation of the energy levels of the triplet intraligand (^{3}IL) excited state and the triplet ligand-to-ligand charge transfer (^{3}LLCT) excited state, which plays important roles in the activation of the TADF behavior of the gold(III) complexes, thus affecting the EL performance of their OLEDs. Particularly, the activation of TADF is observed in the complexes with 4-(diphenylamino)aryl and phosphine oxide as the substituents of the carbazolyl ligands. Furthermore, the excited state lifetime can be significantly reduced by more than two orders of magnitude, *i.e.* from ∼80 μs to 0.8 μs upon changing from the cyano moiety to the 4-(diphenylamino)aryl unit in the ancillary ligand. In addition, the steric effect of different substituents would also affect the rigidity of the molecules and the extent of preferential alignment. These complexes have been found to exhibit high photoluminescence quantum yields (PLQYs) of 80% in solid-state thin films. Green-to yellow-emitting vacuum-deposited and solution-processed OLEDs have been achieved based on these complexes with maximum EQEs of 15.0% and 11.7%; more importantly, by turning on TADF, the efficiency roll-offs have been significantly reduced from 65% down to 1% for the solution-processed devices.

Results and discussion

Synthesis, characterization and thermal stability of carbazolylgold(III) complexes

The respective carbazolyl ligands for **1–6** were prepared from either 2-bromo-9*H*-carbazole or 3-bromo-9*H*-carbazole. 3-Cyano-9*H*-carbazole was synthesized by cyanation of 3-bromo-9*H*-carbazole with a stoichiometric amount of copper(I) cyanide,[47] while 3-(diphenylphosphoryl)-9*H*-carbazole was synthesized by the palladium catalyzed P–C cross-coupling reaction between diphenylphosphine oxide and 3-bromo-9*H*-carbazole.[48] The 4-(diphenylamino)aryl-substituted carbazolyl ligands were synthesized by the Suzuki–Miyaura cross-coupling reaction with palladium catalyzed C–C bond formation between 2- or 3-bromo-9*H*-carbazole and the corresponding 4-(diphenylamino)aryl boronic acids.[49] All complexes were synthesized by reacting the corresponding carbazolyl ligands with the chlorogold(III) precursor in the presence of a stoichiometric amount of sodium hydride in tetrahydrofuran solution (see Scheme S1†).[43] The identities of the complexes have been confirmed by ^{1}H, ^{13}C{^{1}H} and ^{31}P{^{1}H} nuclear magnetic resonance (NMR) spectroscopies and high-resolution electrospray ionization mass spectrometry. In order to examine the thermal stability of this series of complexes, all complexes were investigated using the thermogravimetric analysis (TGA) method, with high decomposition temperatures (T_d) of above 380 °C (see Fig. S1†).

Electrochemistry

The electrochemical properties of all the complexes have been investigated by cyclic voltammetry in dichloromethane solution (0.1 M ^{n}Bu$_4$NPF$_6$). The cyclic voltammograms of the oxidation and reduction scans of **1–6** are shown in Fig. S2,† while the electrochemical data of **1–6** are summarized in Table S1.† In general, all the complexes display an irreversible reduction wave at −1.65 V to −1.73 V *vs.* saturated calomel electrode (SCE). With reference to the previously reported carbazolylgold(III) complexes, these irreversible reduction waves are assigned as the cyclometalating C^C^N ligand-centered reduction.[43,44] On the other hand, an irreversible oxidation wave at +0.87 V to +1.20 V *vs.* SCE is found for **1**, **2**, **5** and **6** while a quasi-reversible first oxidation wave at +0.67 V and +0.70 V *vs.* SCE is found for **3** and **4**. The first oxidation process is found to be sensitive to the carbazolyl ligands and thus is assigned as the carbazolyl ligand-centered oxidation.[43,44] With the incorporation of electron-accepting cyano and phosphine oxide moieties, the highest occupied molecular orbital (HOMO) is found to be stabilized, resulting in more positive potentials for oxidation [*i.e.* **1** (+1.20 V *vs.* SCE) and **2** (+1.05 V *vs.* SCE)]. On the other hand, the potentials for oxidation of **3** and **4** are less positive due to the destabilization of the HOMO in the presence of electron-donating 4-(diphenylamino)phenyl moieties. It is worth noting that the potentials for oxidation of **5** and **6** [*i.e.* **5** (+0.87 V *vs.* SCE) and **6** (+0.86 V *vs.* SCE)] are very close to that of the previously reported unsubstituted carbazolylgold(III) complex, [Au{4-^{t}BuC^C(4-^{t}BuC$_6$H$_4$)^N}(Cbz)] (+0.86 V *vs.* SCE).[43] The electron-donating effects of the 4-(diphenylamino)-2-methylphenyl moieties in **5** and **6** are not apparent, possibly due to the weak communication between the carbazolyl and 4-(diphenylamino)aryl moieties at the 2-position.[50] This results in more positive potentials for oxidation of **5** and **6** when compared to those of **3** and **4** [*i.e.* **3** (+0.67 V *vs.* SCE) and **4** (+0.70 V *vs.* SCE)] with the 4-(diphenylamino)aryl moieties incorporated at the 3-position of carbazole.

Photophysical properties

The UV-vis absorption spectra of all the complexes are recorded in toluene at 298 K, as shown in Fig. S3,† while the absorption data are summarized in Table S2.† All the complexes show an intense absorption band at *ca.* 310–350 nm and a less intense absorption shoulder at *ca.* 360–400 nm, with extinction coefficients (ε) on the order of 10^3 dm^3 mol^{-1} cm^{-1}. Additionally, all the complexes show an absorption band which extends to *ca.* 450–550 nm. With reference to the previously reported carbazolylgold(III) complexes,[43] the absorption bands with wavelength (λ) ≤ 350 nm for **1** and **2** are attributed to the spin-allowed IL $\pi \rightarrow \pi^*$ transitions of the C^C^N ligand, while those for **3–6** are attributed to the spin-allowed IL $\pi \rightarrow \pi^*$ transitions of the C^C^N ligand and the 4-(diphenylamino)aryl moiety. The less intense absorption shoulders of **1–6** are tentatively assigned as an admixture of metal-perturbed IL $\pi \rightarrow \pi^*$ transitions of the C^C^N ligand with some charge-transfer character from the phenyl ring to the pyridine ring, while the absorption tails of **1–6** are tentatively assigned as the ligand-to-ligand charge transfer (LLCT) π[carbazole] $\rightarrow \pi^*$[C^C^N] transitions. Considering the low-energy LLCT transitions, **1** and **2** show an apparent blue-shifted absorption tail when compared to **3–6**, [*i.e.* **2** (445 nm); **3–6** (∼460 nm)], due to a lower-lying HOMO level arising from the stabilization by the electron-accepting moieties on the carbazolyl ligands of **1** and **2**. The slightly red-shifted absorption

tails of **3** and **4** when compared to those of **5** and **6**, [*i.e.* **3** and **4** (~465 nm); **5** and **6** (~455 nm)], arise from the more destabilized HOMO levels, which are in good agreement with the electrochemical studies.

Fig. 1a depicts the normalized photoluminescence (PL) spectra of **1–6** in degassed toluene at 298 K, while Table 1 summarizes their luminescence data. Upon excitation at $\lambda \geq$ 365 nm, all the complexes display intense structureless emission bands with emission maxima at *ca.* 540–660 nm. The emission bands are assigned as originating from the LLCT π [carbazole] → π*[C^C^N] state.[43] The emission energies of **5** and **6** are found to be close to that of the previously reported complex, [Au{4-^{t}BuC^C(4-^{t}BuC$_6$H$_4$)^N}(Cbz)], *i.e.*, **5** (600 nm) and **6** (599 nm) ≈ [Au{4-^{t}BuC^C(4-^{t}BuC$_6$H$_4$)^N}(Cbz)] (607 nm) > **3** (659 nm) and **4** (637 nm), which agrees well with the trend of the HOMO–LUMO gaps obtained from the electrochemical study. To further confirm these assignments, nanosecond transient absorption (TA) measurements have been performed on representative complexes **1** and **6** in degassed toluene at room temperature (Fig. 2 and S4,† respectively). Both complexes display a moderately intense positive band at *ca.* 365 nm in the TA spectra, which is assigned to the absorption of the radical anion of the cyclometalating C^C^N ligand, similar to those of the tridentate cyclometalated ligand-containing gold(III) complexes reported previously.[51] Meanwhile, the moderately intense positive band at *ca.* 535 nm for **1** and the less intense positive band at *ca.* 630 nm for **6** are assigned to the absorption of the carbazolyl radical cations of **1** and **6**, respectively. These are in good agreement with the TA spectral traces of related organic carbazole-containing chromophores[52] and carbazole-containing transition metal complexes[53,54] in the literature. The red-shift of the TA band of **6** when compared to **1** is a result of the replacement of the electron-accepting cyano group with the electron-donating 4-(diphenylamino)-2-methylphenyl moiety on the carbazolyl ligand. Furthermore, the TA spectrum of **6** displays a moderately intense low-energy positive band at *ca.* 685 nm, which is assigned to the absorption of the 4-

(diphenylamino)-2-methylphenyl radical cation, similar to those reported for the 4-(diphenylamino)phenyl-containing gold(III) complexes.[51] The absorption decay lifetimes are found to be 1.6 μs at 535 nm and 0.5 μs at 630 nm for **1** and **6**, respectively, which are comparable to their respective emission decay lifetimes in toluene, confirming the assignment of the excited state absorptions of the complexes in toluene.

The emission behavior of these complexes has also been investigated in solid-state thin films, as depicted in the normalized PL spectra of **1–6** in 20 wt% doped *N,N'*-dicarbazolyl-3,5-benzene (MCP) thin films (Fig. 1b). High PLQYs of up to 80% can be observed from the thin films of this series of complexes. It is worth noting that with the incorporation of an extra methyl group *ortho* to the carbazolyl substitution, the PLQYs of **4** and **6** in 10 wt% MCP thin films are higher than those of **3** and **5**, respectively [*i.e.* **4** (0.60) > **3** (0.38) and **6** (0.79) > **5** (0.65)]. The higher PLQYs can be ascribed to the presence of the methyl group *ortho* to the carbazolyl group, which rigidifies the complexes, thus reducing the rate of non-radiative decay. Since the emission band is rather insensitive to the dopant concentration, with only relatively insignificant red shifts on increasing dopant concentration (Fig. S5†), it is unlikely to be mainly resulting from an excimeric emission. In general, the emission behavior of **1–6** in thin films is found to resemble that in the solution state, except that vibronic-structured emission bands are found for **1** and **2**. The rather unsymmetrical band of **2** indicates that there are at least two excited states with rather similar energy levels involved in the emissions, possibly the ^{3}IL excited state of the cyclometalating ligand and the ^{3}LLCT excited state from the carbazolyl ligand to the pyridyl unit, where the energy levels of the ^{3}LLCT excited state can be fine-tuned by changing the substituent on the carbazolyl moiety. The presence of two excited states can also be supported by the time-resolved emission spectra of **2** in the 20 wt% doped MCP thin film (Fig. 3a), where the time-delayed emission spectra show a change in emission band shape from the rather featureless unsymmetric band in the prompt emission
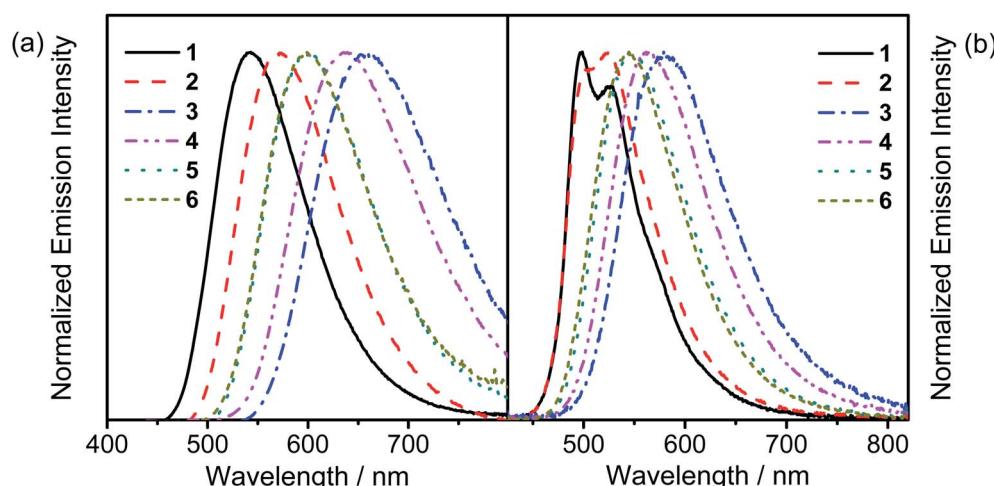

Fig. 1 (a) Normalized PL spectra of **1–6** in degassed toluene at 298 K. (b) Normalized PL spectra of thin films of 20 wt% **1–6** doped in MCP at 298 K.

**Table 1** Luminescence data of the gold(III) complexes

Complex	Medium (T/K)	Emission λ_{em}/nm (τ_o/μs)	$\Phi_{soln}{}^a$	$\Phi_{film}{}^b$	$k_r{}^c$/s^{-1}	$k_{nr}{}^c$/s^{-1}
1	Toluene (298)	540 (2.0)	0.15		7.50×10^4	4.25×10^5
	Solid (298)	497, 544				
	Solid (77)	509, 543, 591				
	Glass (77)^d	484, 518, 556, 608 (233.5)				
	Thin film (298)					
	5 wt% in MCP^e	494, 524 (81.6)		0.41	5.02×10^3	7.23×10^3
	10 wt% in MCP^e	495, 525 (78.9)		0.40	5.07×10^3	7.60×10^3
	15 wt% in MCP^e	497, 526 (67.0)		0.41	6.12×10^3	8.81×10^3
	20 wt% in MCP^e	498, 526 (62.9)		0.34	5.41×10^3	1.05×10^4
2	Toluene (298)	570 (0.6)	0.14		2.33×10^5	1.43×10^6
	Solid (298)	512, 542 (5.9, 49)^f				
	Solid (77)	522, 559, 605 (24.6, 131.2)^f				
	Glass (77)^d	484, 520, 560, 607 (199.6)				
	Thin film (298)					
	5 wt% in MCP^e	496, 523 (70.4)		0.57	8.10×10^3	6.11×10^3
	10 wt% in MCP^e	497, 523 (64.6)		0.63	9.75×10^3	5.73×10^3
	15 wt% in MCP^e	499, 523 (59.4)		0.60	1.01×10^4	6.73×10^3
	20 wt% in MCP^e	501, 524 (54.7)		0.59	1.08×10^4	7.50×10^3
3	Toluene (298)	659 (0.04)	0.003		6.98×10^4	2.32×10^7
	Solid (298)	608				
	Solid (77)	588				
	Glass (77)^d	563 (2.2)				
	Thin film (298)					
	5 wt% in MCP^e	557 (1.7)		0.44	2.59×10^5	3.29×10^5
	10 wt% in MCP^e	568 (1.2)		0.38	3.17×10^5	5.17×10^5
	15 wt% in MCP^e	568 (1.1)		0.36	3.28×10^5	5.82×10^5
	20 wt% in MCP^e	580 (0.8)		0.27	3.38×10^5	9.13×10^5
4	Toluene (298)	637 (0.1)	0.01		1.00×10^5	9.90×10^6
	Solid (298)	595				
	Solid (77)	570				
	Glass (77)^d	481, 548 (1.8, 3.6)^f				
	Thin film (298)					
	5 wt% in MCP^e	546 (2.9)		0.60	2.07×10^5	1.38×10^5
	10 wt% in MCP^e	554 (2.0)		0.60	3.00×10^5	2.00×10^5
	15 wt% in MCP^e	560 (1.6)		0.56	3.50×10^5	2.75×10^5
	20 wt% in MCP^e	564 (1.3)		0.52	4.00×10^5	3.69×10^5
5	Toluene (298)	600 (0.5)	0.05		1.00×10^5	1.90×10^6
	Solid (298)	542				
	Solid (77)	527, 566				
	Glass (77)^d	481, 516, 553 (4.0, 8.9)^f				
	Thin film (298)					
	5 wt% in MCP^e	530 (12.7)		0.63	4.96×10^4	2.91×10^4
	10 wt% in MCP^e	537 (10.2)		0.65	6.37×10^4	3.43×10^4
	15 wt% in MCP^e	539 (7.2)		0.68	9.44×10^4	4.44×10^4
	20 wt% in MCP^e	548 (4.8)		0.66	1.38×10^5	7.08×10^4
6	Toluene (298)	599 (0.5)	0.07		1.20×10^5	1.88×10^6
	Solid (298)	517, 556				
	Solid (77)	527, 560				
	Glass (77)^d	483, 520, 558 (4.3, 10.6)^f				
	Thin film (298)					
	5 wt% in MCP^e	527 (7.6)		0.76	1.00×10^5	3.16×10^4
	10 wt% in MCP^e	535 (5.9)		0.79	1.34×10^5	3.56×10^4
	15 wt% in MCP^e	538 (4.0)		0.64	1.60×10^5	9.00×10^4
	20 wt% in MCP^e	543 (3.2)		0.68	2.13×10^5	1.00×10^5

^{a} The relative luminescence quantum yield in solution was measured at room temperature using quinine sulphate in 1 N H_2SO_4 as the reference (excitation wavelength = 365 nm, Φ_{soln} = 0.546). ^{b} Φ_{film} of gold(III) complexes doped into 5–20 wt% MCP excited at a wavelength of 320 nm. ^{c} Radiative decay rate constant determined from the equation $k_r = \Phi_{em}/\tau_o$; non-radiative decay rate constant determined from the equation $k_{nr} = (1 - \Phi_{em})/\tau_o$. ^{d} Measured in EtOH–MeOH–CH_2Cl_2 (40 : 10 : 1, v/v). ^{e} Prepared by spin-coating. ^{f} Bi-exponential decay.

spectrum to a more vibronic-structured band, indicating the presence of two close-lying emission origins, with vibronic-structured IL emission having a longer excited-state lifetime that led to the pure vibronic-structured emission band at long time delays. In contrast, only a structureless Gaussian-shape band typical of LLCT origin can be observed in the time-
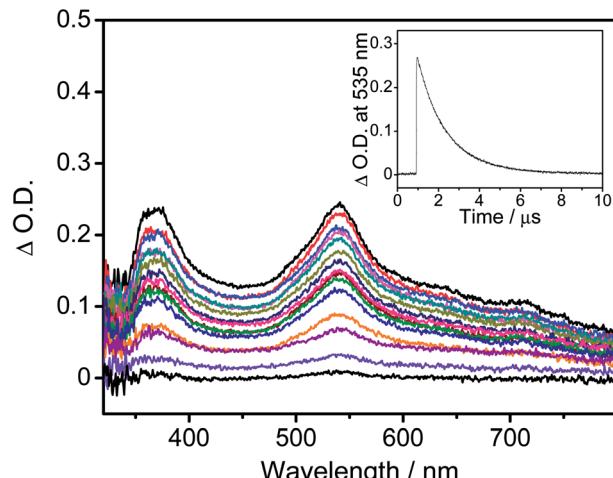
Fig. 2 Transient absorption spectra of **1** in degassed toluene at 298 K at decay times of 0–4 μs and the decay trace monitored at 535 nm in the inset.

resolved emission spectra of **6** in the 20 wt% doped MCP thin film (Fig. 3b) given the lack of the high-energy IL excited state involvement in the emission origin. Similarly, the vibronic-structured emission of **1** in the 20 wt% doped MCP thin film is suggestive of a low-lying ^{3}IL state arising from the presence of the electron-withdrawing cyano substituent on the carbazolyl moiety. Besides the electronic effect that led to the change in excited state origin, the steric effect imposed by the bulky 4-(diphenylamino)aryl substituent over the less sterically demanding cyano group would also rigidify the complex and affect the molecular orientation, especially with the 4-(diphenylamino)-2-methylphenyl moiety instead of the cyano moiety as a substituent. The presence of steric effect has also been reported to play an important role in molecular orientation, thus influencing the outcoupling efficiency.[46]

Computational studies

To gain a deeper understanding into the nature and energies of the excited states of these complexes, density functional theory (DFT) and time-dependent density functional theory (TDDFT) calculations have been performed on **1**, **2** and **6**. The optimized ground-state (S$_0$) geometries and the selected structural parameters of these complexes are shown in Fig. S6.† The first fifteen singlet excited states of **1**, **2** and **6** are summarized in Table S3,† and the simulated UV-vis spectra, generated by Multiwfn,[55] are shown in Fig. S7–S9.† Selected molecular orbitals involved in the transitions are shown in Fig. S10–S12.† The S$_0$ → S$_1$ transitions correspond to the HOMO → LUMO excitation in **1** and **2**, and the HOMO − 1 → LUMO excitation in **6**. For all the complexes, the HOMO and HOMO − 1 are predominantly the π orbitals localized on the carbazolyl ligand, while the LUMOs are the π* orbitals predominantly localized on the central phenyl ring and the pyridine moiety of the C^C^N ligand. Hence, the absorption tail is assigned as the LLCT [π(carbazolyl ligand) → π*(C^C^N)] transition, which supports the experimental energy trend of the absorption tails and their spectral assignments. The orbital energy diagram showing the frontier molecular orbitals of **1**, **2** and **6** is shown in Fig. S13.† The HOMO energy levels are found to be sensitive to the substituents of the carbazolyl ligand, *i.e.* **1** < **2** < **6** where the electron-accepting strengths of the substituents decrease, whereas the LUMO energies are less affected, in good agreement with the experimental trend. Through manipulating the substituents, the HOMO–LUMO gap which corresponds to the LLCT transition energy can be fine-tuned (*i.e.* **1** > **2** > **6**).

TADF properties

In order to investigate whether these gold(III) complexes show TADF behavior, the emission properties of the thin films of **6** have been studied at various temperatures, with Fig. 4a depicting the variable-temperature emission spectra of **6** in 20 wt% doped thin films from 160–300 K. Significant growth in luminescence intensity has been observed upon increasing the temperature. Meanwhile, the solid-state emission of **2** is found to be blue-shifted from 77 to 298 K (Fig. 4b). As TADF compounds are well known to show luminescence intensity growth and blue-shifted emission with increasing temperature and behave just like other TADF-active gold(III) complexes
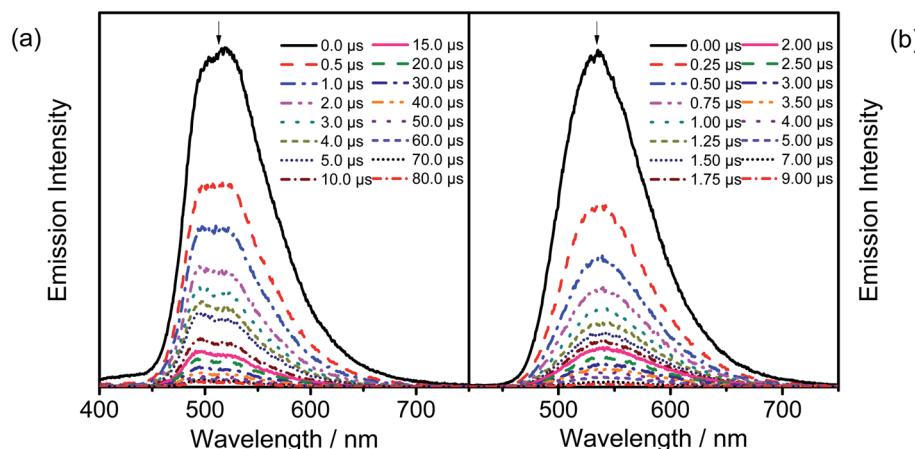
Fig. 3 Time-resolved emission spectra of (a) **2** and (b) **6** doped at 20 wt% in MCP.
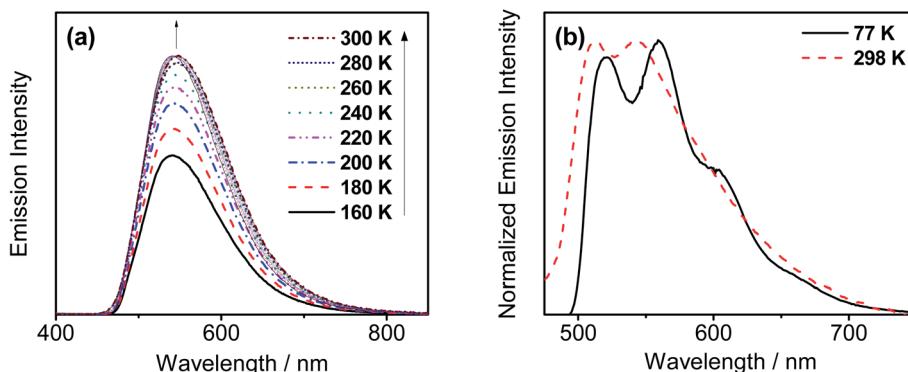
Fig. 4 (a) Emission spectra of 20 wt% **6** doped in the MCP thin film upon increasing the temperature from 160 to 300 K. (b) Normalized PL spectra of the solid sample of **2** at 77 and 298 K.

previously reported,[35,36] it is likely that **2** and **6** could possibly be TADF emitters. Yet the experimental ΔE_{ST} cannot be obtained since the non-radiative decay is not negligible[56] and the excited state lifetimes show insignificant changes in the achievable temperature range.[57]

In view of the experimental limitations, further scrutiny using DFT and TDDFT calculations has been made on **1**, **2** and **6** to investigate the possible involvement of TADF in the excited states. As shown in the natural transition orbitals (NTO) (Fig. S14–S16†), for the S_1 and T_1 states of **2** and **6**, and the S_1 state of **1**, the highest occupied NTOs (HONTO) are predominantly the π orbitals localized on the carbazolyl ligand, whereas the lowest unoccupied NTO (LUNTO) is mainly localized on the C^C^N ligand, revealing the $^{1/3}$LLCT character of these states. On the other hand, both the HONTO and the LUNTO of the T_1 state of **1** are localized on the C^C^N ligand, indicating the ^{3}IL character. This indicates that the judicious choices of the substituents can manipulate the ^{3}IL and ^{3}LLCT excited states by fine-tuning the HOMO energy levels of the gold(III) complexes. For instance, the strongly electron-accepting cyano group can stabilize the π orbitals of the carbazolyl moiety of **1**, resulting in a lower-lying ^{3}IL excited state
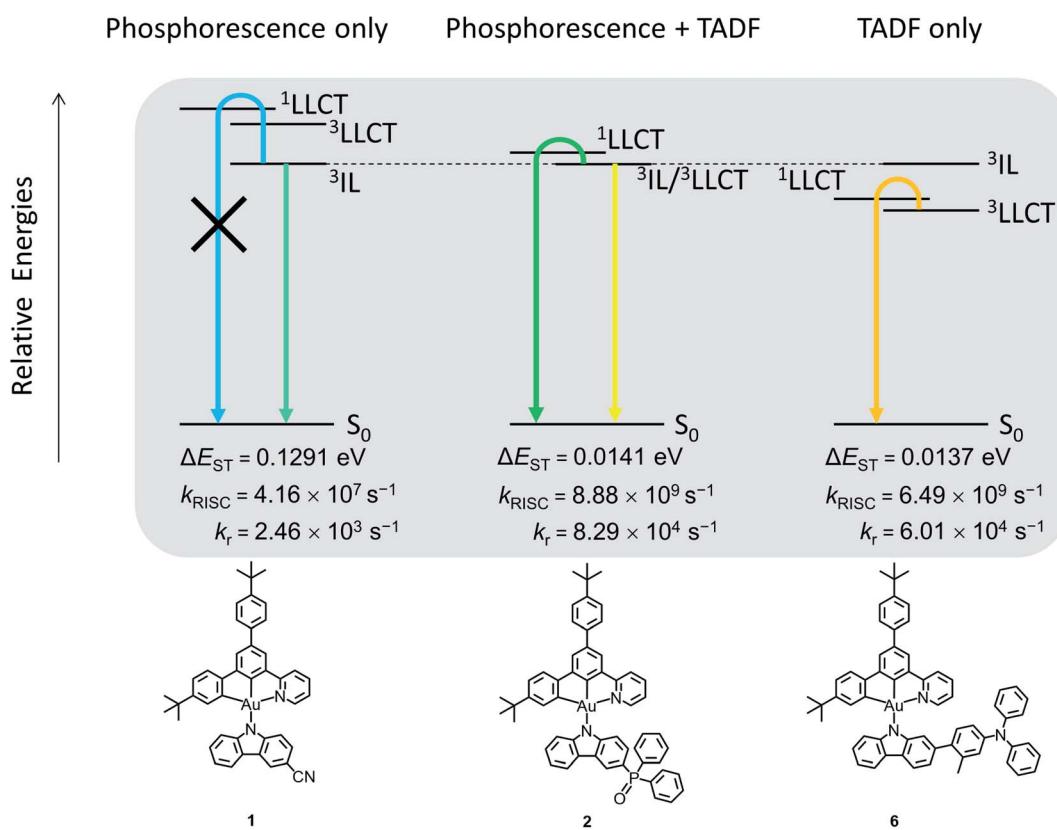
Fig. 5 Relative energies of the excited states involved in the emission (*i.e.* ^{3}IL, ^{3}LLCT and ^{1}LLCT) of **1**, **2** and **6**.

than the ^{3}LLCT excited state. The relatively less electron-accepting phosphine oxide moiety stabilizes the π orbitals of the carbazolyl moiety of **2** to a smaller extent, and therefore the ^{3}LLCT and ^{3}IL excited states share similar energy. Meanwhile, the π orbitals of the carbazolyl moiety of **3–6** are destabilized due to the presence of electron-donating 4-(diphenylamino)aryl moieties, such that their ^{3}LLCT excited states are lower-lying than the ^{3}IL excited states. The relative energies of these excited states of **1**, **2** and **6** are depicted in Fig. 5.

To further investigate the TADF properties of the complexes, the geometries of **1**, **2** and **6** at S_1 and T_1 excited states are optimized, and the rate of radiative decay (k_r), energy between singlet and triplet states (ΔE_{ST}) and the rate of reverse inter-system crossing (k_{RISC}) are summarized in Fig. 5. The ΔE_{ST} values of **2** and **6** are significantly smaller than that of **1** [**2** and **6** (~0.0140 eV) < **1** (0.1291 eV)]. The small ΔE_{ST} values of **2** and **6** indicate the feasible occurrence of TADF at ambient temperature, while it is very unlikely for **1** to show TADF due to the much larger ΔE_{ST}. Furthermore, the k_{RISC} values of **2** and **6** are much larger than that of **1** [**2** (8.88×10^9 s^{-1}), **6** (6.49×10^9 s^{-1}) > **1** (4.16×10^7 s^{-1})], indicating the more efficient RISC for **2** and **6**, which is critical for them to exhibit TADF, while the smaller k_{RISC} of **1** does not favor the occurrence of TADF. Together with experimental results mentioned previously, **1** likely behaves as a phosphorescence emitter, while **2** and **6** can behave as TADF emitters (see Fig. 5). **2** shows dual emission that originates from both ^{1}LLCT and ^{3}IL excited states, owing to the close-lying energy of the ^{3}LLCT and ^{3}IL excited states. The involvement of ^{3}IL excited states is supported by the significantly longer excited state lifetimes of **2** of several tens of microseconds in the thin film state. Meanwhile, the emission of **6** likely originates from TADF from upconversion to the ^{1}LLCT excited state, supported by the shorter excited state lifetimes of only a few microseconds. This agrees well with both the experimental and calculated k_r, in which the k_r values of both **2** and **6** are larger than that of **1** (see Fig. 5 and Table 1), which is the result of the activation of TADF of **2** and **6**, providing an extra radiative decay channel that **1** does not have. On the other hand, based on the trend of the relative energies of excited states being affected by the substituents for **1**, **2** and **6**, this series of complexes is likely to be TADF active if the substituents are less electron-accepting than the phosphine oxide moiety. Therefore, complexes **3–5**, that contain 4-(diphenylamino)aryl moieties as substituents, are expected to show TADF behavior. It can be concluded that the relative energies of ^{3}IL and ^{3}LLCT excited states are crucial for the activation of TADF, and the manipulation of substituents on the carbazolyl ligand can serve as a simple but effective way to control the on/off switching of TADF behavior, providing insights into the future design of TADF-gold(III) materials.

Molecular orientation studies

In light of the recent interest in enhancing outcoupling of the emission through the preferential horizontal orientation of emitters,[58] angular-dependent PL experiments have been carried out on the vacuum-deposited thin films of 11% v/v **6** doped in 3,3′-di(9H-carbazol-9-yl)-1,1′-biphenyl (m-CBP). m-CBP
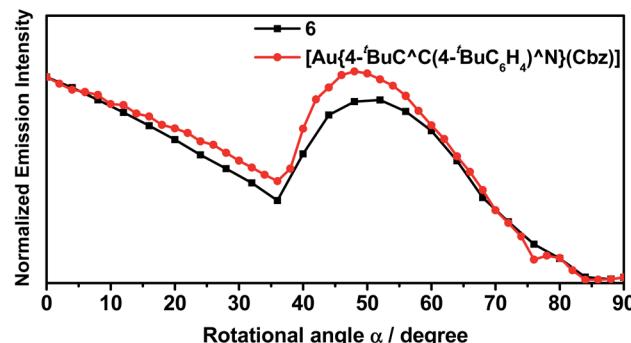
Fig. 6 Angular-dependent PL intensities of the p-polarized light of **6** and [Au{4-^{t}BuC^C(4-^{t}BuC$_6$H$_4$)^N}(Cbz)] (11% v/v) in m-CBP thin films with 20 nm thickness.

has been selected as the host to ensure that the preferential orientation is solely induced by the gold(III) emitters, given that m-CBP remains in a random orientation in a wide range of deposition temperatures.[59] As shown in Fig. 6 and Table S13,† the order parameter S is found to be −0.16 for **6**. Given that S ranges from −0.5 as perfect horizontal orientation to +1.0 as vertically aligned orientation, where $S = 0$ indicates a random molecular orientation,[60] $S = −0.16$ for **6** indicates that the molecules of **6** prefer to be more inclined toward horizontal alignment in the host matrix. It is worth noting that **6** bears an additional 4-(diphenylamino)-2-methylphenyl moiety on the carbazolyl ligand when compared to [Au{4-^{t}BuC^C(4-^{t}BuC$_6$H$_4$)^N}(Cbz)]. In contrast to [Au{4-^{t}BuC^C(4-^{t}BuC$_6$H$_4$)^N}(Cbz)], where S is found to be −0.04,[46] the more negative value of S in **6** suggests that the presence of the bulky 4-(diphenylamino)-2-methylphenyl moiety on the carbazolyl ancillary ligand can favor a more extended molecular interaction between **6** and the host matrix, resulting in a more preferential orientation for molecules of **6** to align horizontally.

OLED fabrication and characterization

Both solution-processed and vacuum-deposited OLEDs have been prepared to examine the EL properties of this class of gold(III) complexes. Fig. 7 shows the normalized EL spectra and EQEs of the solution-processed devices based on **1–6** and Tables S14 and S15† summarize their key parameters. Apparently, all the EL spectra resemble the PL spectra, going from a rather unsymmetric vibronic-structured emission band for **1** and **2** to structureless emission for **3–6**. This observation suggests the change of excited states for emission from ^{3}IL to LLCT, which aligns with the assignment in the emission and computational studies. All the solution-processed devices exhibit satisfactory performance with maximum current efficiencies ranging from 15.4 to 38.0 cd A^{-1}, corresponding to maximum EQEs ranging from 6.1 to 11.7%. The discrepancies on device efficiencies are in line with the PLQYs of the complexes in MCP thin films. The maximum EQE of **4** is apparently higher than that of **3** [EQE: **4** (10.0%) > **3** (6.1%)], which is clearly reflected from the difference in their PLQYs [PLQY: **4** (0.60) > **3** (0.38)]. This can be attributed to the reduced non-radiative decay rate due to the relatively larger energy gap [**4** (576 nm) > **3** (584 nm)], and more
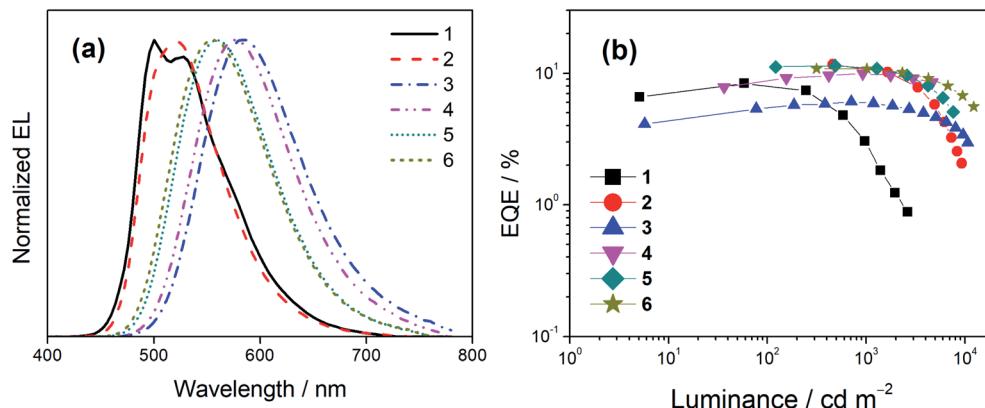
Fig. 7 (a) Normalized EL spectra and (b) EQEs of the solution-processed devices based on **1–6**.

importantly the rigidified molecular structure in the presence of the methyl substituent in **4**, which can restrict the rotation of the 4-(diarylamino)phenyl group at the 3-position of the carbazolyl ligand. Meanwhile, the EQEs of **5** and **6** are found to be fairly similar and the PLQY of **5** is slightly lower than that of **6**, [**5** (0.65) < **6** (0.79)]. The slightly higher PLQY of **6** than **5** could be attributed to the steric effect exerted by the methyl group in **6**, which is less apparent in the EQE measurement. On the other hand, it should be highlighted that the change of excited state origins not only determines the shape of EL spectra, but also has significant impact on the efficiency roll-offs of the devices. Notably, except for **1**, extremely small efficiency roll-offs ($\Delta_{\text{roll-off}}$) from 8% for **2** down to 1% for **4** have been achieved at a luminance of 1000 cd m^{-2}, much smaller than that for the device made with **1** (*i.e.* 65%). The $\Delta_{\text{roll-off}}$ values of these devices are also smaller than that of **1** at a luminance of 5000 cd m^{-2}.

A similar phenomenon has also been observed in the vacuum-deposited OLEDs. Particularly, **2**, **4**, **5** and **6** were utilized to prepare the vacuum-deposited devices. Apart from **2** having two resolved emission bands, other complexes, *i.e.* **4**, **5** and **6**, demonstrate structureless EL spectra (Fig. S17a†). In addition, high current efficiencies of up to 46.4 cd A^{-1} and EQEs of up to 15.0% have been achieved (Fig. S17b and Table S16†). Meanwhile, the operational stabilities of the vacuum-deposited OLEDs were tested under a driving current density of 20 mA cm^{-2}. Fig. S18† depicts the relative luminance of the vacuum-deposited devices as a function of operational time and Table S17† summarizes their lifetime data. Operational half-lifetimes (LT$_{50}$) of up to 2760 hours have been achieved with the device based on **4**. Table S18† summarizes the representative TADF-based OLEDs with similar Commission Internationale de L'Eclairage (CIE) coordinates as **6** for references. Although there is still room for improvement on the operational stability of these TADF-based devices, the present findings demonstrate the effectiveness of ligand manipulation on activating the TADF behavior of gold(III) complexes.

Conclusion

In summary, a new class of cyclometalated C^C^N carbazolylgold(III) complexes has been designed and synthesized

through the incorporation of different electron-donating and electron-accepting moieties at the 2- and 3-positions of the ancillary ligand. By changing cyano to 4-(diphenylamino)aryl moieties in the carbazolyl ligand, the energy levels of the excited states can be manipulated, thus activating TADF for the gold(III) complex. This can effectively reduce the emission lifetime in the gold(III) complexes by more than two orders of magnitude from ~80 μs to 0.8 μs. Together with high PLQYs of up to 80%, efficient solution-processed and vacuum-deposited OLEDs have been obtained. Specifically, $\Delta_{\text{roll-off}}$ of the solution-processed devices can be significantly suppressed when TADF is activated, *i.e.* from 65% in **1** (phosphorescence-based) down to 1% in **4** (TADF-based) at a practical brightness of 1000 cd m^{-2}. This work not only presents the design principles for the manipulation of the excited state nature of the gold(III) complexes through functionalizing the carbazolyl ligand, but also demonstrates the strategy to reduce the detrimental TTA effect in the gold(III)-based OLEDs by activating the TADF behavior.

Data availability

The datasets supporting this article have been uploaded as part of the ESI.†

Author contributions

V. W.-W. Y. initiated and designed the research. V. W.-W. Y., M.-C. T., L.-K. L. and C.-Y. W. designed the gold(III) complexes. C.-Y. W. conducted the synthesis, characterization, photophysical and electrochemical measurements of the gold(III) complexes. M.-Y. L., W.-K. T., and M. N. performed and analyzed the computational calculations. S.-L. L., W.-L. C. and M.-Y. C. carried out the OLED fabrication and characterizations. V. W.-W. Y. supervised the work. All authors discussed the results and contributed to the manuscript.

Conflicts of interest

The authors declare no competing financial interest.

Acknowledgements

References

1 C. W. Tang and S. A. VanSlyke, Organic Electroluminescent Diodes, *Appl. Phys. Lett.*, 1987, **51**, 913.

2 B. W. D'Andrade and S. R. Forrest, White Organic Light-Emitting Devices for Solid-State Lighting, *Adv. Mater.*, 2004, **16**, 1585.

3 S. R. Forrest, The Path to Ubiquitous and Low-Cost Organic Electronic Appliances on Plastic, *Nature*, 2004, **428**, 911.

4 L. Xiao, Z. Chen, B. Qu, J. Luo, S. Kong, Q. Gong and J. Kido, Recent Progresses on Materials for Electrophosphorescent Organic Light-Emitting Devices, *Adv. Mater.*, 2011, **23**, 926.

5 H. Uoyama, K. Goushi, K. Shizu, H. Nomura and C. Adachi, Highly Efficient Organic Light-Emitting Diodes from Delayed Fluorescence, *Nature*, 2012, **492**, 234.

6 D. V. Khramtchenkov, H. Bässler and V. I. Arkhipov, A Model of Electroluminescence in Organic Double-Layer Light-Emitting Diodes, *J. Appl. Phys.*, 1996, **79**, 9283.

7 J. Kalinowski, W. Stampor, J. Mężyk, M. Cocchi, D. Virgili, V. Fattori and P. Di Marco, Quenching Effects in Organic Electrophosphorescence, *Phys. Rev. B: Condens. Matter Mater. Phys.*, 2002, **66**, 235321.

8 N. C. Giebink and S. R. Forrest, Quantum Efficiency Roll-Off at High Brightness in Fluorescent and Phosphorescent Organic Light Emitting Diodes, *Phys. Rev. B: Condens. Matter Mater. Phys.*, 2008, **77**, 235215.

9 C. Murawski, K. Leo and M. C. Gather, Efficiency Roll-Off in Organic Light-Emitting Diodes, *Adv. Mater.*, 2013, **25**, 6801.

10 C. S. Oh, H. L. Lee, S. H. Han and J. Y. Lee, Rational Molecular Design Overcoming the Long Delayed Fluorescence Lifetime and Serious Efficiency Roll-Off in Blue Thermally Activated Delayed Fluorescent Devices, *Chem.–Eur. J.*, 2019, **25**, 642.

11 Y. Sun and S. R. Forrest, High-Efficiency White Organic Light Emitting Devices with Three Separate Phosphorescent Emission Layers, *Appl. Phys. Lett.*, 2007, **91**, 263503.

12 Y. Sun and S. R. Forrest, Multiple Exciton Generation Regions in Phosphorescent White Organic Light Emitting Devices, *Org. Electron.*, 2008, **9**, 994.

13 H. Sasabe, J. Takamatsu, T. Motoyama, S. Watanabe, G. Wagenblast, N. Langer, O. Molt, E. Fuchs, C. Lennartz and J. Kido, High-Efficiency Blue and White Organic Light-Emitting Devices Incorporating a Blue Iridium Carbene Complex, *Adv. Mater.*, 2010, **22**, 5003.

14 M. A. Baldo, S. Lamansky, P. E. Burrows, M. E. Thompson and S. R. Forrest, Very High-Efficiency Green Organic Light-Emitting Devices Based on Electrophosphorescence, *Appl. Phys. Lett.*, 1999, **75**, 4.

15 D. F. O'Brien, M. A. Baldo, M. E. Thompson and S. R. Forrest, Improved Energy Transfer in Electrophosphorescent Devices, *Appl. Phys. Lett.*, 1999, **74**, 442.

16 D. S. M. Ravinson and M. E. Thompson, Thermally Assisted Delayed Fluorescence (TADF): Fluorescence Delayed is Fluorescence Denied, *Mater. Horiz.*, 2020, **7**, 1210.

17 M. Z. Shafikov, A. F. Suleymanova, R. Czerwieniec and H. Yersin, Design Strategy for Ag(I)-Based Thermally Activated Delayed Fluorescence Reaching an Efficiency Breakthrough, *Chem. Mater.*, 2017, **29**, 1708.

18 B. Pashaei, S. Karimi, H. Shahroosvand, P. Abbasi, M. Pilkington, A. Bartolotta, E. Fresta, J. Fernandez-Cestau, R. D. Costa and F. Bonaccorso, Polypyridyl Ligands as a Versatile Platform for Solid-State Light-Emitting Devices, *Chem. Soc. Rev.*, 2019, **48**, 5033.

19 R. Czerwieniec, J. Yu and H. Yersin, Blue-Light Emission of Cu(I) Complexes and Singlet Harvesting, *Inorg. Chem.*, 2011, **50**, 8293.

20 Z. Liu, M. F. Qayyum, C. Wu, M. T. Whited, P. I. Djurovich, K. O. Hodgson, B. Hedman, E. I. Solomon and M. E. Thompson, A Codeposition Route to CuI–Pyridine Coordination Complexes for Organic Light-Emitting Diodes, *J. Am. Chem. Soc.*, 2011, **133**, 3700.

21 X.-L. Chen, R. Yu, Q.-K. Zhang, L.-J. Zhou, X.-Y. Wu, Q. Zhang and C.-Z. Lu, Rational Design of Strongly Blue-Emitting Cuprous Complexes with Thermally Activated Delayed Fluorescence and Application in Solution-Processed OLEDs, *Chem. Mater.*, 2013, **25**, 3910.

22 G. Li, Z.-Q. Zhu, Q. Chen and J. Li, Metal Complex Based Delayed Fluorescence Materials, *Org. Electron.*, 2019, **69**, 135.

23 M. Osawa, M. Hoshino, M. Hashimoto, I. Kawata, S. Igawa and M. Yashima, Application of Three-Coordinate Copper(I) Complexes with Halide Ligands in Organic Light-Emitting Diodes that Exhibit Delayed Fluorescence, *Dalton Trans.*, 2015, **44**, 8369.

24 D. Volz, Y. Chen, M. Wallesch, R. Liu, C. Fléchon, D. M. Zink, J. Friedrichs, H. Flügge, R. Steininger, J. Göttlicher, C. Heske, L. Weinhardt, S. Bräse, F. So and T. Baumann, Bridging the Efficiency Gap: Fully Bridged Dinuclear Cu(I)-Complexes for Singlet Harvesting in High-Efficiency OLEDs, *Adv. Mater.*, 2015, **27**, 2538.

25 Z.-Q. Zhu, T. Fleetham, E. Turner and J. Li, Harvesting All Electrogenerated Excitons through Metal Assisted Delayed Fluorescent Materials, *Adv. Mater.*, 2015, **27**, 2533.

26 Z.-Q. Zhu, C.-D. Park, K. Klimes and J. Li, Highly Efficient Blue OLEDs Based on Metal-Assisted Delayed Fluorescence Pd(II) Complexes, *Adv. Opt. Mater.*, 2019, **7**, 1801518.

27 A. S. Romanov, S. T. E. Jones, L. Yang, P. J. Conaghan, D. Di, M. Linnolahti, D. Credgington and M. Bochmann, Mononuclear Silver Complexes for Efficient Solution and Vacuum-Processed OLEDs, *Adv. Opt. Mater.*, 2018, **6**, 1801347.

28 M. Z. Shafikov, A. F. Suleymanova, A. Schinabeck and H. Yersin, Dinuclear Ag(I) Complex Designed for Highly Efficient Thermally Activated Delayed Fluorescence, *J. Phys. Chem. Lett.*, 2018, **9**, 702.

29 T. Teng, K. Li, G. Cheng, Y. Wang, J. Wang, J. Li, C. Zhou, H. Liu, T. Zou, J. Xiong, C. Wu, H.-X. Zhang, C.-M. Che and C. Yang, Lighting Silver(I) Complexes for Solution-Processed Organic Light-Emitting Diodes and Biological Applications *via* Thermally Activated Delayed Fluorescence, *Inorg. Chem.*, 2020, **59**, 12122.

30 D. Di, A. S. Romanov, L. Yang, J. M. Richter, J. P. H. Rivett, S. Jones, T. H. Thomas, M. A. Jalebi, R. H. Friend, M. Linnolahti, M. Bochmann and D. Credgington, High-Performance Light-Emitting Diodes Based on Carbene-Metal-Amides, *Science*, 2017, **356**, 159.

31 J. M. López-de-Luzuriaga, M. Monge, M. E. Olmos, M. Rodríguez-Castillo, I. Soldevilla, D. Sundholm and R. R. Valiev, Perhalophenyl Three-Coordinate Gold(I) Complexes as TADF Emitters: A Photophysical Study from Experimental and Computational Viewpoints, *Inorg. Chem.*, 2020, **59**, 14236.

32 W.-P. To, D. Zhou, G. S. M. Tong, G. Cheng, C. Yang and C.-M. Che, Highly Luminescent Pincer Gold(III) Aryl Emitters: Thermally Activated Delayed Fluorescence and Solution-Processed OLEDs, *Angew. Chem., Int. Ed.*, 2017, **56**, 14036.

33 D. Zhou, W.-P. To, Y. Kwak, Y. Cho, G. Cheng, G. S. M. Tong and C.-M. Che, Thermally Stable Donor–Acceptor Type (Alkynyl)Gold(III) TADF Emitters Achieved EQEs and Luminance of up to 23.4% and 70 300 cd m^{-2} in Vacuum-Deposited OLEDs, *Adv. Sci.*, 2019, **6**, 1802297.

34 D. Zhou, W.-P. To, G. S. M. Tong, G. Cheng, L. Du, D. L. Phillips and C.-M. Che, Tetradentate Gold(III) Complexes as Thermally Activated Delayed Fluorescence (TADF) Emitters: Microwave-Assisted Synthesis and High-Performance OLEDs with Long Operational Lifetime, *Angew. Chem., Int. Ed.*, 2020, **59**, 6375.

35 C. C. Au-Yeung, L.-K. Li, M.-C. Tang, S.-L. Lai, W.-L. Cheung, M. Ng, M.-Y. Chan and V. W.-W. Yam, Molecular Design of Efficient Yellow- to Red-Emissive Alkynylgold(III) Complexes for the Realization of Thermally Activated Delayed Fluorescence (TADF) and Their Applications in Solution-Processed Organic Light-Emitting Devices, *Chem. Sci.*, 2021, **12**, 9516.

36 L.-K. Li, W.-K. Kwok, M.-C. Tang, W.-L. Cheung, S.-L. Lai, M. Ng, M.-Y. Chan and V. W.-W. Yam, Highly Efficient Carbazolylgold(III) Dendrimers Based on Thermally Activated Delayed Fluorescence and Their Application in Solution-Processed Organic Light-Emitting Devices, *Chem. Sci.*, 2021, **12**, 14833.

37 L.-K. Li, C. C. Au-Yeung, M.-C. Tang, S.-L. Lai, W.-L. Cheung, M. Ng, M.-Y. Chan and V. W.-W. Yam, Design and Synthesis of Yellow- to Red-Emitting Gold(III) Complexes Containing Isomeric Thienopyridine and Thienoquinoline Moieties and Their Applications in Operationally Stable Organic Light-Emitting Devices, *Mater. Horiz.*, 2022, **9**, 281.

38 V. W.-W. Yam, K. M.-C. Wong, L.-L. Hung and N. Zhu, Luminescent Gold(III) Alkynyl Complexes: Synthesis, Structural Characterization, and Luminescence Properties, *Angew. Chem., Int. Ed.*, 2005, **44**, 3107.

39 K. M.-C. Wong, X. Zhu, L.-L. Hung, N. Zhu, V. W.-W. Yam and H.-S. Kwok, A Novel Class of Phosphorescent Gold(III) Alkynyl-Based Organic Light-Emitting Devices with Tunable Colour, *Chem. Commun.*, 2005, 2906.

40 V. K.-M. Au, K. M.-C. Wong, D. P.-K. Tsang, M.-Y. Chan, N. Zhu and V. W.-W. Yam, High-Efficiency Green Organic Light-Emitting Devices Utilizing Phosphorescent Bis-Cyclometalated Alkynylgold(III) Complexes, *J. Am. Chem. Soc.*, 2010, **132**, 14273.

41 M.-C. Tang, D. P.-K. Tsang, M. M.-Y. Chan, K. M.-C. Wong and V. W.-W. Yam, Dendritic Luminescent Gold(III) Complexes for Highly Efficient Solution-Processable Organic Light-Emitting Devices, *Angew. Chem., Int. Ed.*, 2013, **52**, 446.

42 M.-C. Tang, M.-Y. Leung, S.-L. Lai, M. Ng, M.-Y. Chan and V. W.-W. Yam, Realization of Thermally Stimulated Delayed Phosphorescence in Arylgold(III) Complexes and Efficient Gold(III) Based Blue-Emitting Organic Light-Emitting Devices, *J. Am. Chem. Soc.*, 2018, **140**, 13115.

43 L.-K. Li, M.-C. Tang, S.-L. Lai, M. Ng, W.-K. Kwok, M.-Y. Chan and V. W.-W. Yam, Strategies Towards Rational Design of Gold(III) Complexes for High-Performance Organic Light-Emitting Devices, *Nat. Photonics*, 2019, **13**, 185.

44 W.-K. Kwok, M.-C. Tang, S.-L. Lai, W.-L. Cheung, L.-K. Li, M. Ng, M.-Y. Chan and V. W.-W. Yam, Judicious Choice of *N*-Heterocycles for the Realization of Sky-Blue- to Green-Emitting Carbazolylgold(III) C^C^N Complexes and Their Applications for Organic Light-Emitting Devices, *Angew. Chem., Int. Ed.*, 2020, **59**, 9684.

45 B. Y.-W. Wong, H.-L. Wong, Y.-C. Wong, M.-Y. Chan and V. W.-W. Yam, Versatile Synthesis of Luminescent Tetradentate Cyclometalated Alkynylgold(III) Complexes and Their Application in Solution-Processable Organic Light-Emitting Devices, *Angew. Chem., Int. Ed.*, 2017, **56**, 302.

46 M.-C. Tang, L.-K. Li, S.-L. Lai, W.-L. Cheung, M. Ng, C.-Y. Wong, M.-Y. Chan and V. W.-W. Yam, Design Strategy Towards Horizontally Oriented Luminescent Tetradentate-Ligand-Containing Gold(III) Systems, *Angew. Chem., Int. Ed.*, 2020, **59**, 21023.

47 G. P. Ellis and T. M. Romney-Alexander, Cyanation of Aromatic Halides, *Chem. Rev.*, 1987, **87**, 779.

48 O. Berger, C. Petit, E. L. Deal and J.-L. Montchamp, Phosphorus-Carbon Bond Formation: Palladium-Catalyzed Cross-Coupling of H-Phosphinates and Other P(O)H-Containing Compounds, *Adv. Synth. Catal.*, 2013, **355**, 1361.

49 P. Kochapradist, N. Prachumrak, R. Tarsang, T. Keawin, S. Jungsuttiwong, T. Sudyoadsuk and V. Promarak, Multi-Triphenylamine-Substituted Carbazoles: Synthesis,

Characterization, Properties, and Applications as Hole-Transporting Materials, *Tetrahedron Lett.*, 2013, **54**, 3683.

50 S. Kato, H. Noguchi, S. Jin and Y. Nakamura, Synthesis and Electronic, Optical, and Electrochemical Properties of a Series of Tetracyanobutadiene-Substituted Carbazoles, *Asian J. Org. Chem.*, 2016, **5**, 246.

51 V. K.-M. Au, D. P.-K. Tsang, K. M.-C. Wong, M.-Y. Chan, N. Zhu and V. W.-W. Yam, Functionalized Bis-Cyclometalated Alkynylgold(III) Complexes: Synthesis, Characterization, Electrochemistry, Photophysics, Photochemistry, and Electroluminescence Studies, *Inorg. Chem.*, 2013, **52**, 12713.

52 L. M. Lifshits, D. S. Budkina, V. Singh, S. M. Matveev, A. N. Tarnovsky and J. K. Klosterman, Solution-State Photophysics of *N*-Carbazolyl Benzoate Esters: Dual Emission and Order of States in Twisted Push–Pull Chromophores, *Phys. Chem. Chem. Phys.*, 2016, **18**, 27671.

53 C.-H. Lee, M.-C. Tang, F. K.-W. Kong, W.-L. Cheung, M. Ng, M.-Y. Chan and V. W.-W. Yam, Isomeric Tetradentate Ligand-Containing Cyclometalated Gold(III) Complexes, *J. Am. Chem. Soc.*, 2019, **142**, 520.

54 Y.-J. Cho, S.-Y. Kim, M. R. Son, H.-J. Son, D. W. Cho and S. O. Kang, Time-Resolved Spectroscopic Analysis of the Light-Energy Harvesting Mechanism in Carbazole-Dendrimers with a Blue-Phosphorescent Ir-Complex Core, *Phys. Chem. Chem. Phys.*, 2017, **19**, 20093.

55 T. Lu and F. Chen, Multiwfn: A Multifunctional Wavefunction Analyzer, *J. Comput. Chem.*, 2012, **33**, 580.

56 R. Hamze, S. Shi, S. C. Kapper, D. S. Muthiah Ravinson, L. Estergreen, M.-C. Jung, A. C. Tadle, R. Haiges, P. I. Djurovich, J. L. Peltier, R. Jazzar, G. Bertrand, S. E. Bradforth and M. E. Thompson, "Quick-Silver" from a Systematic Study of Highly Luminescent, Two-Coordinate, d^{10} Coinage Metal Complexes, *J. Am. Chem. Soc.*, 2019, **141**, 8616.

57 F. B. Dias, T. J. Penfold and A. P. Monkman, Photophysics of Thermally Activated Delayed Fluorescence Molecules, *Methods Appl. Fluoresc.*, 2017, **5**, 012001.

58 K.-H. Kim and J.-J. Kim, Origin and Control of Orientation of Phosphorescent and TADF Dyes for High-Efficiency OLEDs, *Adv. Mater.*, 2018, **30**, 1705600.

59 T. Komino, H. Tanaka and C. Adachi, Selectively Controlled Orientational Order in Linear-Shaped Thermally Activated Delayed Fluorescent Dopants, *Chem. Mater.*, 2014, **26**, 3665.

60 D. Yokoyama, Molecular Orientation in Small-Molecule Organic Light-Emitting Diodes, *J. Mater. Chem.*, 2011, **21**, 19187.